Novel magnetic resonance antennas and applications

Ruytenberg, T.

Author: Ruytenberg, T.
Title: Novel magnetic resonance antennas and applications
Issue Date: 2020-06-04

1

General Introduction

T. Ruytenberg

1

1.1. THE WIDER PERSPECTIVE

In health care, medical imaging has become an ever more used diagnostic tool [1–3]. Not only have medical imaging techniques become more available in the developed world [4], also imaging capabilities per modality have increased due to technological advances. In magnetic resonance imaging (MRI) specifically, during the last decades increasing static magnetic field strengths, the invention of acceleration algorithms, advanced radio frequency (RF) antenna design, and the increase in computation power for reconstruction of images have brought many advances in increasing the quality and resolution of MRI images. This thesis will focus on the topic of RF antenna and antenna array design and in this introduction the role of RF antennas in MRI and some important design criteria are covered.

1.2. RF COILS IN MRI

Using MRI, spin systems can be studied by creating a net magnetization in a sample using a large magnet and subsequently perturbing it out of its equilibrium state and measuring the precession frequency of the system. MRI systems are most used in clinical practise to image humans for diagnostic purposes utilizing static magnetic field strengths in the order of Tesla (T). This static magnetic field is called the B_0 field.

Once a magnetization has been established in the sample, the system can be probed using a second time-dependent magnetic field at the Larmor precession frequency. This field is named the B_1 field, and by looking at the gyromagnetic ratio for protons $\gamma = 42.58\,\mathrm{MHzT^{-1}}$, given the B_0 field strengths used in clinical practise, one easily calculates that the working frequencies are in the radio frequency range and therefore to be applied and detected with radio antennas. During an experiment a transmit B_1 field is applied and receive B_1 field is measured via the radio antenna, for which often the term 'coil' is used. It is an important notion that these transmit and receive fields are not necessarily identical.

Due to the precession of the spins, the B_1 fields are polarized circularly [5]. Fields acting on the spin system and fields generated by the spin system are therefore oppositely polarized. We can therewith define the two fields separately if the direction of the B_0 field is defined [6]

$$\mathbf{B_0} = B_0\hat{\mathbf{z}} \tag{1.1}$$

$$\mathbf{B_1} = \hat{\mathbf{x}}B_{1x} + \hat{\mathbf{y}}B_{1y} + \hat{\mathbf{z}}B_{1z} \tag{1.2}$$

$$\mathbf{B_1^+} = (\hat{\mathbf{x}} + j\hat{\mathbf{y}})\mathbf{B_1}/\sqrt{2} \tag{1.3}$$

$$\mathbf{B_1^-} = (\hat{\mathbf{x}} - j\hat{\mathbf{y}})\mathbf{B_1}/\sqrt{2} \tag{1.4}$$

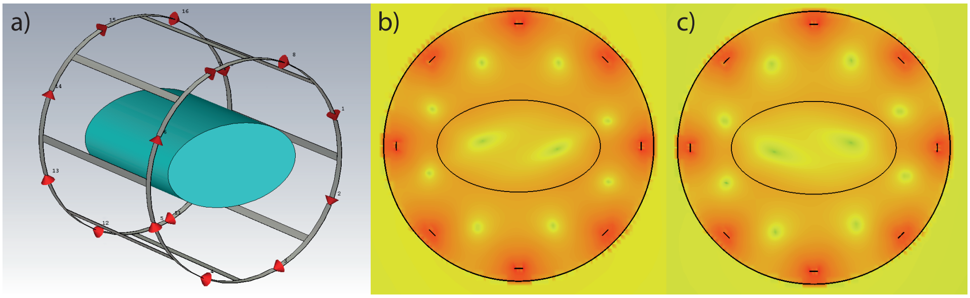

Figure 1.1: A birdcage coil and its produced fields in a phantom. a) birdcage coil drawn in simulation software, showing the birdcage with the red cones being discrete ports simulated as capacitors including a total of two driving ports. (shield around coil not shown for visibility) b) and c) the simulated B_1^+ and B_1^- fields, showing asymmetry. The phantom has an electric permittivity of $\varepsilon_r = 60$ and conductivity of $\sigma = 1.0\,\mathrm{S/m}$

where B_1^+ is the transmit field and B_1^- the receive field.

A convenient way to produce and detect these circularly polarized fields, also called quadrature excitation or detection [7], was found by Hayes et al. [8] in 1985 with the creation of the birdcage coil (see Figure 1.1a). Essentially an annular multi-loop coil with shared conductors and a single, or two driving channels in the case of quadrature excitation. The birdcage coil has become the working horse in MRI and is incorporated in every 1.5 and 3.0 T system as a body coil. The birdcage has the advantage of being able to produce a rather homogeneous B_1 field.

While the transmit and receive fields differ in polarization, additionally the field distribution can vary spatially throughout the sample due to secondary magnetic fields created by induced currents in the sample via Maxwell's law with Ampère's addition

$$\nabla \times \mathbf{B_1} = \mu_0 \mathbf{J_c} + \mu_0 \mathbf{J_d} = \mu_0(\sigma + \varepsilon_0 \varepsilon_r j\omega)\mathbf{E} \tag{1.5}$$

with $\mathbf{J_c}$ the conduction current and $\mathbf{J_d}$ the displacement current. Note that the secondary magnetic fields become larger at higher frequencies (or field strengths) and higher conductivities of the sample. Thereby also the asymmetry between the transmit and receive field will increase, depicted in Figure 1.1b and c. Additional examples of asymmetry at different field strengths have for example been published by Vaidya et al. [9].

1

1.3. DESIGN CONSIDERATIONS

RECEIVE-ONLY COILS

Even though the birdcage coil is often used in clinical MRI due to its large volume coverage with rather homogeneous B_1 fields, it is not very reasonably sensitive on the receive side, as the coil is up to tens of centimeters away from the region of interest to be imaged and the signals to be measured are small in the order of milliwatt. A method for substantially increasing the signal-to-noise ratio (SNR) was described in detail by Hoult [5] in 1978 for applications in NMR. By splitting the transmit and receive chain, one can use the body coil as homogeneous transmitter and a separate receive-only coil close to the region of interest. For an extended region of interest though, one would have to move the receive coil around to compensate for the limited FOV (field of view) of such a coil. A solution to extend the FOV would be to create an array of multiple adjacent receive loop coils and a working setup incorporating this idea in MRI was presented in 1990 by Roemer [10].

The difficulties arising from making an array of coils in MRI originate from the fact that the separate elements in such an array are in each others electromagnetic near-field. Therefore, a coupling exists between these elements. As MRI functions with narrow-band resonators as antennas, one obtains a system of damped coupled resonators for which only system-wide modes are present. These new coupled modes are not at the original resonant frequency of the single uncoupled elements anymore, resulting in an off-resonance antenna, useless for MRI.

Roemer solved this issue by compensating the initial coupling by introducing additional coupling between elements in the form of overlap. By overlapping elements, additional magnetic flux from one element to the other is induced, but with an opposite sign. This way the total inductive coupling cancels out between neighbouring elements if done precisely. For next-nearest neighbours this decoupling method does not work, as no overlap can be created between these elements.

Nowadays, receive-only coils are universally used when working with clinical MRI scanners. Head coils often consist of 32 or more elements, while body arrays are growing towards 128 or even more elements. In general more elements will result in a higher surface SNR, while central SNR depends more on the total array coverage[i] [11–14]. Many of these multi-element arrays depend on overlap for reducing most of their coupling between neighbouring elements.

While overlapping elements is generally very effective for loop coils, the decoupling can be compromised under varying loading conditions of the coil, can be less or more effective at different field strengths [15, 16], and the method cannot be applied to coils with very different geometries than loops. Different methods to decouple elements within an

[i]Going to extremes in number of elements may tip the balance from gaining additional signal with extra channels, to a built-up of coil noise, reducing total SNR.

array have been extensively described. For example, introducing additional resonating circuits between elements [17–21], adjusting current distributions [22, 23], intrinsic geometric decoupling if different coil types are used [24], preamplifier decoupling[ii] [10] and the use of high impedance coils [27].

With the presence of receive-arrays in MRI, algorithms to accelerate imaging, like SMASH [28], SENSE [29] and GRAPPA [30] were introduced in 1997, 1999 and 2002 respectively. Additionally to the practical problem of shifting resonances that arises from inter-element coupling in an array as discussed previously, these algorithms also degrade under high amounts of coupling. Even though the mathematical approaches to these methods are not very difficult to follow, only the intuitive way of their working is briefly touched upon here, as they are intuitively easy to comprehend and the math has been written down before in the referenced work. The methods described in this paragraph all rely on the fact that one obtains virtually free additional information when scanning with an array. When a scan is performed with an n-channel array, n-times more data is acquired compared to the single channel coil. Combined with knowledge that the individual elements within the array are only sensitive within their own immediate surrounding, free spatial encoding is obtained when using an array at the only cost of sampling multiple channels. An n-channel array would therefore theoretically allow for an acceleration of n, as in that case the same amount of data is sampled.

However, for this to work perfectly, the sensitivities of the individual channels need to be unique and non-overlapping. In the mathematical approach this manifests itself as the noise correlation matrix of the channels. If two channels show correlation in their noise, they are partly sampling the same MRI signal either because these channels both have sensitivity for the same voxel, or because MRI signal is picked up by a channel and directly coupled into another channel via the electronics. Whichever of the underlying coupling pathways occur, they both result in non-unique channels, thereby slightly spoiling the acceleration method in the form of spatially-dependent noise amplification in the accelerated images. Where exactly in the images the noise will be amplified therefore depends on the total scan setup, composed of the array geometry, the object geometry and the acceleration factor being used. The noise amplification is therefore also called the geometry factor and for a pixel p it is in the SENSE algorithm given by [29]

$$g_p = \sqrt{[(S^H \Psi^{-1} S)^{-1}]_{p,p} (S^H \Psi^{-1} S)_{p,p}} \geq 1 \tag{1.6}$$

with S being a vector with all the pixel intensities per channel, H indicating the Hermitian transpose and Ψ the noise correlation matrix. A properly decoupled array shows low geometry factors for high accelerations and using a SENSE acceleration factor of R will show the following SNR

[ii] Although preamplifier decoupling eases construction of arrays, SNR gains have been disputed if the combination of channels is done with proper weightings [25, 26]

1

$$SNR_p^{SENSE} = \frac{SNR_p^{FULL}}{g_p\sqrt{R}} \tag{1.7}$$

compared to the fully sampled SNR case. A properly decoupled array therefore not only shows a low g-factor, but therefore also directly increases SNR when using accelerated scanning.

TRANSMIT-ONLY COILS

With the introduction of receive-only coils in this chapter, one obviously still needs a transmitter to excite the spin system and this can be either a transmit-only, or a transceive coil. In clinical practise, often the large body (birdcage) coil is used, but in some specific cases transmit arrays are chosen. When designing transmit coils, not only transmit efficiency is important in design, especially the safety aspects have to be considered as in the order of kilowatts of RF power is applied using these antennas resulting in E-field induced heating, also called the specific absorption rate (SAR). While transmit efficiency can easily be measured, as it concerns an applied B-field. E-field induced heating however, is not easily measured in-situ[iii]. Therefore heating is often simulated using finite-difference time-domain simulations and these simulations have become much more important with the use of transmit coil arrays close to the body, not only due to their potentially high local E-fields, but also due to their dependency of the phase settings per transmit channel. When an array is driven with a set of phases for the different channels, constructive interference can occur in a certain region within the subject, while it might not for another set of phases [33].

An example of how some coils have evolved through time considering these transmit design criteria can be seen with the dipole-type antennas [34–36]. These coils are more often used to replace or complement [24, 35–37] loop coil arrays for field strengths beyond 3 T. Their efficiency at high-field is sometimes explained by their generated current patterns adhering more to the ideal current patterns needed for optimum SNR [38, 39]. The continued work on dipoles has led to small adaptations in geometry such as folding, bumping, fractionating and meandering [39–42], inversion via Babinet's principle [43] to slots [44] and passively fed dipoles [45], most of them with the intention to improve transmit efficiency and to reduce E-field induced heating.

ARRAY DESIGN CRITERIA

For receive-only arrays it is important to consider:

- Inter-element decoupling

[iii] A single indirect method to measure temperature increase with MRI is well-described in literature, based on the proton resonance frequency temperature-dependency [31, 32].

- Decoupling from the transmit coil
- The total amount of elements and their arrangement as this influences acceleration performance and surface SNR
- The amount of surface coverage to obtain sufficient central SNR for the application

For transmit-only/transceive arrays additionally:

- Known E-field-induced heating characteristics
- Components should be chosen such that they can handle the intended power levels

Indubitably, safety is of the utmost importance when putting a coil into use. Besides safety on the RF side, mechanical safety, electrical safety and flammability of the coil should be considered. [33]

1.4. HIGH PERMITTIVITY MATERIALS

MRI is a well-coordinated play between the spin system under study (often a human being) and the antenna-system as exciters and as sensor. The mediator between these two is the electromagnetic field, which is bound by the properties of the whole system and especially the subject in the case of MRI, as it has a non-vacuum electric permittivity. Implications of this non-vacuum, and at the same time frequency-dependent, permittivity are well-known and understood and have its largest impact at ultra-high field MRI where it manifests as B_1-field inhomogeneity [46, 47]. This is also where the first application of high permittivity materials presents itself, to perturb the B_1^+-field, such to obtain an increased or more homogeneous transmit field in an anatomy or region of interest [48–50].

Another application can (simultaneously) be found on the receive side, where additionally sensitivities can be enhanced [50, 51], which will also be the subject of Chapter 5.

Other uses of dielectric materials include for example dielectric resonators [52–56]. By exciting an electromagnetic mode of the resonators, and having the imaging region of interest close to or even inside the maximum of the H-field of this mode, imaging sensitivities can be enhanced. Also in the area of implant safety, dielectric materials may have its benefits [57].

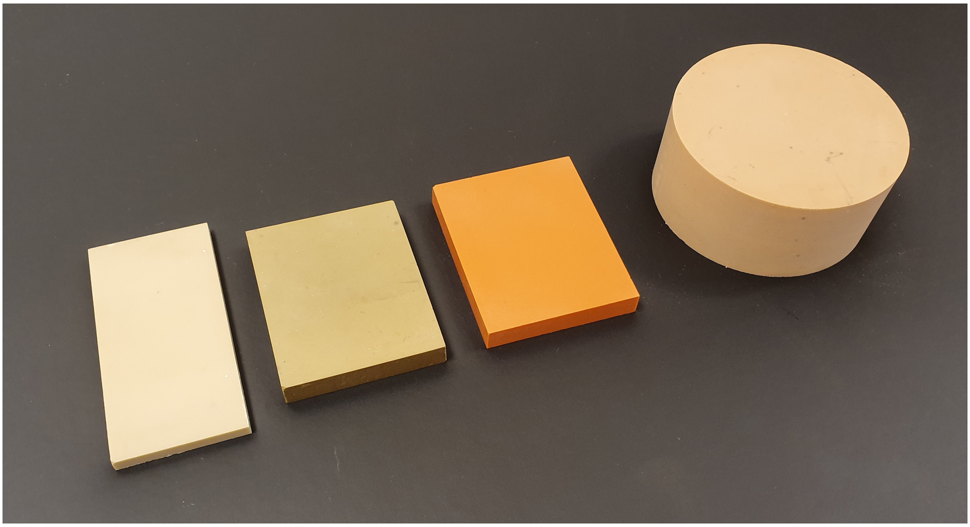

Figure 1.2: A variety of solid high permittivity material used in MRI. From left to right: lead zirconate titanate (ε_r = 1070 and σ = 1.5 S/m) used in Chapter 4, lead zirconate titanate (ε_r = 660 and σ = 0.01 S/m) used in Chapter 5, barium titanate with zirconium dioxide and ceric dioxide additives (ε_r = 4500 and σ = 1.79 S/m) used in Reference [45] and barium strontium titanate (ε_r = 165) used in Reference [58]

1.5. THIS WORK

The work described in this thesis covers a range of surface coil designs, partly using high permittivity materials, and their applications.

Chapter 2 demonstrates high resolution laryngeal imaging using a semi-flexible dedicated coil. While clinical laryngeal scanning is often difficult, both due to artefacts of swallowing and breathing, and due to low sensitivity of generally used coils for this anatomy, the dedicated coil and the implemented sequences therewith resulted in high quality images of the larynx.

A very flexible transceive and receive-only array was designed in **Chapter 3** using coaxial cable loop antennas. Even though the array is flexible, does not contain any lumped elements in the resonating circuit, and has no inter-element decoupling circuitry, the array shows lower inter-element decoupling than an array of conventional loop coils.

Chapter 4 describes a novel receive-only array of dielectric resonator antennas. When resonant dielectric materials are being used for receive-only purposes, they need to be detuned during the transmit phases when scanning. For these solid dielectric resonators, this was achieved by attaching PIN-diodes to the resonators using conductive silver paint, which resulted in a fully electrically detunable coil with dielectric resonators.

In **Chapter 5** the use of fully integrated high-permittivity material in receive-only coils is described. While the use of high-permittivity materials in MRI have been extensively researched in literature, integrating these materials starting from the design phase had not yet been described. This chapter presents the benefits of doing so by comparing coils constructed for imaging the neck with and without high-permittivity material.

1

REFERENCES

[1] W. R. Hendee, G. J. Becker, J. P. Borgstede, J. Bosma, W. J. Casarella, B. A. Erickson, C. D. Maynard, J. H. Thrall, and P. E. Wallner, *Addressing overutilization in medical imaging,* Radiology **257**, 240 (2010).

[2] R. Smith-Bindman, D. L. Miglioretti, and E. B. Larson, *Rising use of diagnostic medical imaging in a large integrated health system,* Health affairs **27**, 1491 (2008).

[3] R. Smith-Bindman, D. L. Miglioretti, E. Johnson, C. Lee, H. S. Feigelson, M. Flynn, R. T. Greenlee, R. L. Kruger, M. C. Hornbrook, D. Roblin, *et al.*, *Use of diagnostic imaging studies and associated radiation exposure for patients enrolled in large integrated health care systems, 1996-2010,* Jama **307**, 2400 (2012).

[4] Organisation for Economic Co-operation and Development, *Health Statistics 2019: Health Care Utilisation,* `https://stats.oecd.org/`.

[5] D. Hoult, *The NMR receiver: a description and analysis of design,* Progress in Nuclear Magnetic Resonance Spectroscopy **12**, 41 (1978).

[6] T. S. Ibrahim, *Analytical approach to the MR signal,* Magnetic Resonance in Medicine: An Official Journal of the International Society for Magnetic Resonance in Medicine **54**, 677 (2005).

[7] C.-N. Chen, D. Hoult, and V. Sank, *Quadrature detection coils - a further $\sqrt{2}$ improvement in sensitivity,* Journal of Magnetic Resonance (1969) **54**, 324 (1983).

[8] C. E. Hayes, W. A. Edelstein, J. F. Schenck, O. M. Mueller, and M. Eash, *An efficient, highly homogeneous radiofrequency coil for whole-body NMR imaging at 1.5 T,* Journal of Magnetic Resonance (1969) **63**, 622 (1985).

[9] M. V. Vaidya, C. M. Collins, D. K. Sodickson, R. Brown, G. C. Wiggins, and R. Lattanzi, *Dependence of and field patterns of surface coils on the electrical properties of the sample and the MR operating frequency,* Concepts in Magnetic Resonance Part B: Magnetic Resonance Engineering **46**, 25 (2016).

[10] P. B. Roemer, W. A. Edelstein, C. E. Hayes, S. P. Souza, and O. M. Mueller, *The NMR phased array,* Magnetic resonance in medicine **16**, 192 (1990).

[11] G. C. Wiggins, J. R. Polimeni, A. Potthast, M. Schmitt, V. Alagappan, and L. L. Wald, *96-channel receive-only head coil for 3 Tesla: design optimization and evaluation,* Magnetic Resonance in Medicine: An Official Journal of the International Society for Magnetic Resonance in Medicine **62**, 754 (2009).

[12] G. C. Wiggins, C. Triantafyllou, A. Potthast, A. Reykowski, M. Nittka, and L. Wald, *32-channel 3 Tesla receive-only phased-array head coil with soccer-ball element geometry,* Magnetic Resonance in Medicine: An Official Journal of the International Society for Magnetic Resonance in Medicine **56**, 216 (2006).

[13] B. Keil, J. N. Blau, S. Biber, P. Hoecht, V. Tountcheva, K. Setsompop, C. Triantafyllou, and L. L. Wald, *A 64-channel 3T array coil for accelerated brain MRI,* Magnetic resonance in medicine **70**, 248 (2013).

[14] M. Schmitt, A. Potthast, D. E. Sosnovik, J. R. Polimeni, G. C. Wiggins, C. Triantafyllou, and L. L. Wald, *A 128-channel receive-only cardiac coil for highly accelerated cardiac MRI at 3 Tesla,* Magnetic Resonance in Medicine: An Official Journal of the International Society for Magnetic Resonance in Medicine **59**, 1431 (2008).

[15] N. Avdievich, A. Pfrommer, I. Giapitzakis, and A. Henning, *Analytical modeling provides new insight into complex mutual coupling between surface loops at ultrahigh fields,* NMR in Biomedicine **30**, e3759 (2017).

[16] N. I. Avdievich, I.-A. Giapitzakis, A. Pfrommer, and A. Henning, *Decoupling of a tight-fit transceiver phased array for human brain imaging at 9.4 T: Loop overlapping rediscovered,* Magnetic resonance in medicine **79**, 1200 (2018).

[17] N. I. Avdievich, J. W. Pan, and H. P. Hetherington, *Resonant inductive decoupling (RID) for transceiver arrays to compensate for both reactive and resistive components of the mutual impedance,* NMR in Biomedicine **26**, 1547 (2013).

[18] X. Yan, X. Zhang, B. Feng, C. Ma, L. Wei, and R. Xue, *7T transmit/receive arrays using ICE decoupling for human head mr imaging,* IEEE transactions on medical imaging **33**, 1781 (2014).

[19] X. Yan, L. Wei, S. Chu, R. Xue, and X. Zhang, *Eight-channel monopole array using ICE decoupling for human head MR imaging at 7 T,* Applied magnetic resonance **47**, 527 (2016).

[20] Y. Li, Z. Xie, Y. Pang, D. Vigneron, and X. Zhang, *ICE decoupling technique for RF coil array designs,* Medical physics **38**, 4086 (2011).

[21] X. Yan, J. C. Gore, and W. A. Grissom, *New resonator geometries for ICE decoupling of loop arrays,* Journal of Magnetic Resonance **277**, 59 (2017).

[22] X. Yan, J. C. Gore, and W. A. Grissom, *Self-decoupled RF coils,* in *Proceedings 25. Annual Meeting International Society for Magnetic Resonance in Medicine*, Vol. 25 (Honolulu, Hawaii, 2017) p. 0757.

[23] X. Yan, J. C. Gore, and W. A. Grissom, *Multi-row and loopole-type self-decoupled RF coils,* in *Proceedings 26. Annual Meeting International Society for Magnetic Resonance in Medicine*, Vol. 26 (Paris, France, 2018) p. 4271.

[24] M. A. Ertürk, A. J. Raaijmakers, G. Adriany, K. Uğurbil, and G. J. Metzger, *A 16-channel combined loop-dipole transceiver array for 7 Tesla body MRI,* Magnetic resonance in medicine **77**, 884 (2017).

[25] A. Reykowski, C. Saylor, and G. R. Duensing, *Do we need preamplifier decoupling?* in *Proceedings 19. Annual Meeting International Society for Magnetic Resonance in Medicine*, Vol. 19 (Montréal, Canada, 2011) p. 3883.

[26] C. Findeklee, O. Lips, P. Vernickel, C. Leussler, and R. Duensing, *Preamp decoupling improves SNR and the earth is flat,* in *Proceedings 27. Annual Meeting International Society for Magnetic Resonance in Medicine,* Vol. 27 (Montréal, Canada, 2019) p. 0563.

[27] B. Zhang, D. K. Sodickson, and M. A. Cloos, *A high-impedance detector-array glove for magnetic resonance imaging of the hand,* Nature biomedical engineering **2**, 570 (2018).

[28] D. K. Sodickson and W. J. Manning, *Simultaneous acquisition of spatial harmonics (SMASH): fast imaging with radiofrequency coil arrays,* Magnetic resonance in medicine **38**, 591 (1997).

[29] K. P. Pruessmann, M. Weiger, M. B. Scheidegger, and P. Boesiger, *SENSE: sensitivity encoding for fast MRI,* Magnetic resonance in medicine **42**, 952 (1999).

[30] M. A. Griswold, P. M. Jakob, R. M. Heidemann, M. Nittka, V. Jellus, J. Wang, B. Kiefer, and A. Haase, *Generalized autocalibrating partially parallel acquisitions (GRAPPA),* Magnetic Resonance in Medicine: An Official Journal of the International Society for Magnetic Resonance in Medicine **47**, 1202 (2002).

[31] J. D. Poorter, C. D. Wagter, Y. D. Deene, C. Thomsen, F. Stahlberg, and E. Achten, *Noninvasive MRI thermometry with the proton resonance frequency (PRF) method: in vivo results in human muscle,* Magnetic resonance in medicine **33**, 74 (1995).

[32] F. F. Simonis, E. T. Petersen, J. J. Lagendijk, and C. A. van den Berg, *Feasibility of measuring thermoregulation during RF heating of the human calf muscle using MR based methods,* Magnetic resonance in medicine **75**, 1743 (2016).

[33] J. Hoffmann, A. Henning, I. A. Giapitzakis, K. Scheffler, G. Shajan, R. Pohmann, and N. I. Avdievich, *Safety testing and operational procedures for self-developed radiofrequency coils,* NMR in Biomedicine **29**, 1131 (2016).

[34] A. Raaijmakers, O. Ipek, D. W. Klomp, C. Possanzini, P. Harvey, J. J. Lagendijk, and C. A. van Den Berg, *Design of a radiative surface coil array element at 7 T: the single-side adapted dipole antenna,* Magnetic resonance in medicine **66**, 1488 (2011).

[35] A. Raaijmakers, P. R. Luijten, and C. A. van Den Berg, *Dipole antennas for ultrahigh-field body imaging: a comparison with loop coils,* NMR in Biomedicine **29**, 1122 (2016).

[36] M. K. Woo, R. L. Lagore, L. DelaBarre, B.-Y. Lee, Y. Eryaman, J. Radder, A. Erturk, G. Metzger, P.-F. van de Moortele, K. Ugurbil, *et al.*, *A 16-channel transceiver loop+ dipole antennas head array for human head imaging at 10.5 T,* in *2017 International Conference on Electromagnetics in Advanced Applications (ICEAA)* (IEEE, 2017) pp. 1649–1652.

[37] B. R. Steensma, M. Luttje, I. J. Voogt, D. W. Klomp, P. R. Luijten, C. A. van den Berg, and A. J. Raaijmakers, *Comparing signal-to-noise ratio for prostate imaging at 7T and 3T,* Journal of Magnetic Resonance Imaging **49**, 1446 (2019).

[38] R. Lattanzi and D. K. Sodickson, *Ideal current patterns yielding optimal signal-to-noise ratio and specific absorption rate in magnetic resonance imaging: computational methods and physical insights,* Magnetic resonance in medicine **68**, 286 (2012).

[39] G. C. Wiggins, B. Zhang, R. Lattanzi, G. Chen, and D. Sodickson, *The electric dipole array: An attempt to match the ideal current pattern for central SNR at 7 Tesla,* in *Proceedings 20. Annual Meeting International Society for Magnetic Resonance in Medicine*, Vol. 20 (Melbourne, Australia, 2012) p. 0541.

[40] A. J. Raaijmakers, M. Italiaander, I. J. Voogt, P. R. Luijten, J. M. Hoogduin, D. W. Klomp, and C. A. van Den Berg, *The fractionated dipole antenna: A new antenna for body imaging at 7 Tesla,* Magnetic resonance in medicine **75**, 1366 (2016).

[41] A. Sadeghi-Tarakameh, A. Torrado-Carvajal, C. Ariyurek, E. Atalar, G. Adriany, G. J. Metzger, R. L. Lagore, L. DelaBarre, A. Grant, P.-F. V. de Moortele, K. Ugurbil, and Y. Eryaman, *Optimizing the topography of transmit coils for SAR management,* in *Proceedings 26. Annual Meeting International Society for Magnetic Resonance in Medicine*, Vol. 26 (Paris, France, 2018) p. 0297.

[42] B. R. Steensma, I. J. Voogt, T. Leiner, P. R. Luijten, J. Habets, D. W. Klomp, C. A. van den Berg, and A. J. Raaijmakers, *An 8-channel Tx/Rx dipole array combined with 16 Rx loops for high-resolution functional cardiac imaging at 7 T,* Magnetic Resonance Materials in Physics, Biology and Medicine **31**, 7 (2018).

[43] C. A. Balanis, *Antenna theory,* 3rd ed. (John Wiley & Sons, Inc., Hoboken, New Jersey, 2005).

[44] L. Alon, R. Lattanzi, K. Lakshmanan, R. Brown, C. M. Deniz, D. K. Sodickson, and C. M. Collins, *Transverse slot antennas for high field MRI,* Magnetic resonance in medicine **80**, 1233 (2018).

[45] I. Zivkovic, C. A. de Castro, and A. Webb, *Design and characterization of an eight-element passively fed meander-dipole array with improved specific absorption rate efficiency for 7 T body imaging,* NMR in Biomedicine , e4106 (2019).

[46] A. Webb, *Dielectric materials in magnetic resonance,* Concepts in magnetic resonance part A **38**, 148 (2011).

[47] W. M. Brink, *Dielectric shimming: exploiting dielectric interactions in High Field MRI*, Ph.D. thesis, Department of Radiology, Leiden University Medical Center (2016).

[48] W. Teeuwisse, W. Brink, K. Haines, and A. Webb, *Simulations of high permittivity materials for 7 T neuroimaging and evaluation of a new barium titanate-based dielectric,* Magnetic resonance in medicine **67**, 912 (2012).

[49] K. Koolstra, P. Börnert, W. Brink, and A. Webb, *Improved image quality and reduced power deposition in the spine at 3 T using extremely high permittivity materials,* Magnetic resonance in medicine **79**, 1192 (2018).

1

[50] S. Rupprecht, C. T. Sica, W. Chen, M. T. Lanagan, and Q. X. Yang, *Improvements of transmit efficiency and receive sensitivity with ultrahigh dielectric constant (uHDC) ceramics at 1.5 T and 3 T,* Magnetic resonance in medicine **79**, 2842 (2018).

[51] G. Carluccio, G. Haemer, M. Vaidya, S. Rupprecht, Q. Yang, and C. M. Collins, *SNR Evaluation for a high-permittivity dielectric helmet-shaped coil former for a 28 channel receive array,* in *Proceedings 26. Annual Meeting International Society for Magnetic Resonance in Medicine*, Vol. 26 (Paris, France, 2018) p. 4405.

[52] K. Haines, T. Neuberger, M. Lanagan, E. Semouchkina, and A. Webb, *High Q calcium titanate cylindrical dielectric resonators for magnetic resonance microimaging,* Journal of Magnetic Resonance **200**, 349 (2009).

[53] S. A. Aussenhofer and A. G. Webb, *Design and evaluation of a detunable water-based quadrature HEM11 mode dielectric resonator as a new type of volume coil for high field MRI,* Magnetic resonance in medicine **68**, 1325 (2012).

[54] S. A. Aussenhofer and A. Webb, *High-permittivity solid ceramic resonators for high-field human MRI,* NMR in Biomedicine **26**, 1555 (2013).

[55] T. P. O'Reilly, T. Ruytenberg, and A. G. Webb, *Modular transmit/receive arrays using very-high permittivity dielectric resonator antennas,* Magnetic resonance in medicine **79**, 1781 (2018).

[56] T. Ruytenberg and A. G. Webb, *Design of a dielectric resonator receive array at 7 Tesla using detunable ceramic resonators,* Journal of Magnetic Resonance **284**, 94 (2017).

[57] Z. Yu, X. Xin, and C. M. Collins, *Potential for high-permittivity materials to reduce local SAR at a pacemaker lead tip during MRI of the head with a body transmit coil at 3 T,* Magnetic resonance in medicine **78**, 383 (2017).

[58] S. Aussenhofer and A. Webb, *An eight-channel transmit/receive array of TE01 mode high permittivity ceramic resonators for human imaging at 7 T,* Journal of Magnetic Resonance **243**, 122 (2014).